Dual-width plasmonic gratings with sub-10 nm gaps for biosensor applications

Stephen J. Bauman[a], Ahmad A. Darweesh[a], Joseph B. Herzog[*,a,b]

[a]Microelectronics-Photonics Program, University of Arkansas, Fayetteville, AR, 72701, USA;
[b]Department of Physics, University. of Arkansas, Fayetteville, AR, 72701, USA;

ABSTRACT

Fabrication of dual-width plasmonic gratings with sub-10 nm gaps has been made possible by a recently developed technique. Studying the effects of various material and geometrical parameters on the optical response of these gratings will prove useful to future fabrication of devices. The ability to tune the widths of both wires in the periodic array allows for optimization of the response based not only on one nanowire geometry, but the hybridization of the two. The structures hold potential to be used as a substrate for surface-enhanced Raman spectroscopy (SERS) in the detection of different chemical analytes, with biosensing as a major area of interest. The ability to tune the structures to different wavelengths makes this a potentially attractive method of fabricating sensor substrates capable of enhancing otherwise weak analyte signals. Here, preliminary computational results are shown for a study of the effects of a SiO_2 layer on the substrate containing a plasmonic grating.

Keywords: Plasmon, nanogap, grating, plasmonic enhancement

1. INTRODUCTION

Plasmons are oscillations of free electrons on the surface of a metal. These electron density waves are created when light is incident on the surface of a metal or a metallic structure, due to the oscillating electric field of propagating light. The study of plasmons, plasmonics, has become a popular area of study for both theoretical understanding and potential application to useful technology. Metallic nanostructures are small enough to allow the formation of resonant plasmon modes or to promote propagating surface plasmons with decay lengths on the order of the structure size. This makes harnessing plasmons more feasible than when using devices above the nanoscale. The near-field electric field confinement caused by plasmons is useful because it causes a local increase in the electric field strength compared to that of the incident light causing the plasmons. This strengthened field can benefit photovoltaic light absorption, spectroscopy signal generation/detection, and other applications.[1–4] Bringing two such nanostructures together until they are separated by a nanogap (less than 100 nm) has been shown to improve the electromagnetic responses of such devices, as the plasmons on either nanostructure become close enough to couple into a hybrid mode.[5,6] This gap enhancement increases nearly exponentially as the width decreases below 10 nm.[7–9] Plasmonic devices with nanogaps have been studied for their potential to interact with incident light in ways that can prove useful to various applications.[10–14]

Periodic structures such as plasmonic gratings of parallel metallic nanowires have been studied to understand their potential benefits as spectroscopy signal enhancement devices.[15–18] These types of structures typically have a single nanowire width that repeats for the entire device, with each structure separated by the same gap width on either side. Fabrication of gratings with multiple structure or gap widths per period is typically more difficult than for standard grating geometries, and so has not been heavily studied. Also, sub-10 nm gaps, which are useful for plasmonics, tend to be difficult to fabricate to date. A recently demonstrated nanomasking fabrication technique has been utilized as outlined by Bauman et al. to create plasmonic grating structures containing both sub-10 nm gaps *and* a dual-width period for the metallic nanostructures.[19] Preliminary fabrication results of such a dual-width geometry are shown in the SEM image in Figure 1.

* Email: jbherzog@uark.edu

Nanoengineering: Fabrication, Properties, Optics, and Devices XIII, edited by Eva M. Campo, Elizabeth A. Dobisz, Louay A. Eldada, Proc. of SPIE Vol. 9927, 992709 · © 2016 SPIE
CCC code: 0277-786X/16/$18 · doi: 10.1117/12.2237764

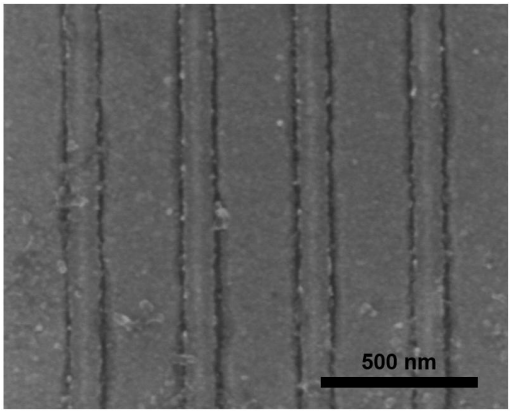

Figure 1. SEM image showing an example of a dual-width grating fabricated via the nanomasking technique.

Preliminary computational studies of such dual-width devices have demonstrated additional optical enhancement effects over that of single width gratings.[20] An example of such results is shown in Figure 2. Here, the optical enhancement $(E/E_0)^2$ is shown for two dual-width instances and one case with only a single structure width per grating period.

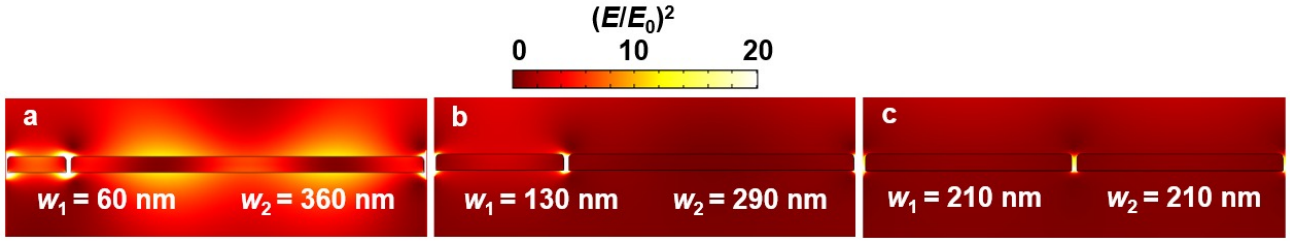

Figure 2. Preliminary results demonstrating the potential benefit of increased optical enhancement provided by a dual-width plasmonic grating ((a) and (b)) compared to a single width grating (c).

In the current work, preliminary results are discussed for simulations of the type plasmonic grating previously described. The optimization of the electromagnetic response of these types of structures is studied with the goal of fabricating substrates for biosensor signal enhancement in mind. The optimization of these grating devices will make use of many separate parametric studies as well as their collaborative results. In conjunction with other geometrical optimization studies involving structure widths, heights, and effects of the adhesion layer, studying the effects of varying the SiO_2 layer thickness on the substrate is important for fabricating useful devices.

2. SILICON DIOXIDE THICKNESS STUDY

The present work has established a finite element method (FEM) model with variable parameters to study the electromagnetic response of the dual-width grating geometry under various conditions. A depiction of the two-dimensional model geometry is shown in Figure 3. The model is established as a cross-section of two infinitely long Au nanostructures separated by a nanogap with periodic boundary conditions on either side to simulate an infinite grating in the horizontal direction. Material properties of Au, Ti, Si, SiO_2, and air are utilized for the applicable regions of the model to simulate the grating structures, Ti adhesion layer, substrate, and grown/native oxide most closely representing the samples capable of being fabricated. For this reason also, the Au structures are beveled with a radius of 5 nm on the top corners. The Au/Ti cross-sectional widths, w_1 and w_2, may be varied independently, as can the gap between them, g, and the heights of all material regions. Thus, the grating period, P, which equals the width of the model, depends on the widths of the structures and the size of the gap between them. In the preliminary results reported here, the gap was held constant at 8 nm, and the Au widths were set equal to one another in order to achieve a baseline for the silicon dioxide thickness study to be performed.

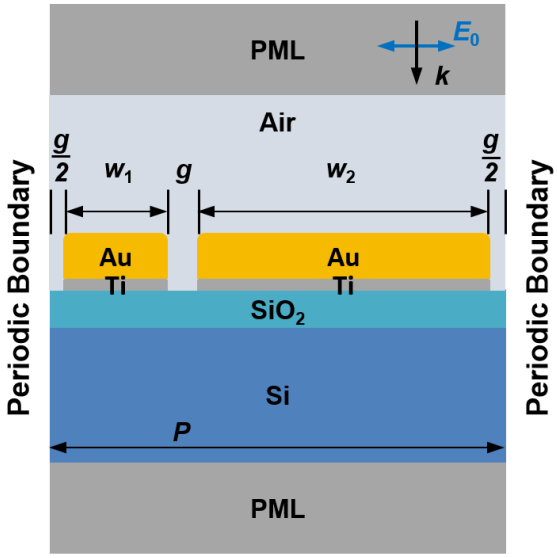

Figure 3. Sketch of the model geometry showing perfectly matched layers and periodic boundary conditions. The regions with different material properties include air, two gold wires with variable widths (w_1 and w_2) on top of titanium layers, a layer of SiO_2, and a bulk Si region. Incident light polarization and propagation directions are represented by E_0 and k, respectively.

The model simulates a plane wave of 785 nm light incident from the top of the model, shown by k, and polarized in the horizontal direction, as shown by E_0 in Figure 3. This wavelength was chosen as it is commonly used for Raman spectroscopy studies. The top and bottom of the model are perfectly matched layers, designed to be perfect absorbers so that light does not scatter back into the model by erroneous interactions at the boundaries. Periodic boundary conditions are implemented at the horizontal edges of the model in order to simulate an infinitely periodic array of the gold stripes with the period equal to the width of the model.

For the preliminary results obtained thus far, the Au widths, $w_1 = w_2 = w$, were swept from 10 to 100 nm for various SiO_2 layer thicknesses, t_{SiO2}, and the summation of the optical enhancement within a small integration box surrounding the gap was calculated. These data are plotted in Figure 4. The goal of this type of simulation is to determine the combinations of geometry, material, and incident wavelength that provide the optimal optical enhancement. This can help focus future device fabrications for experimental verification of these computational results.

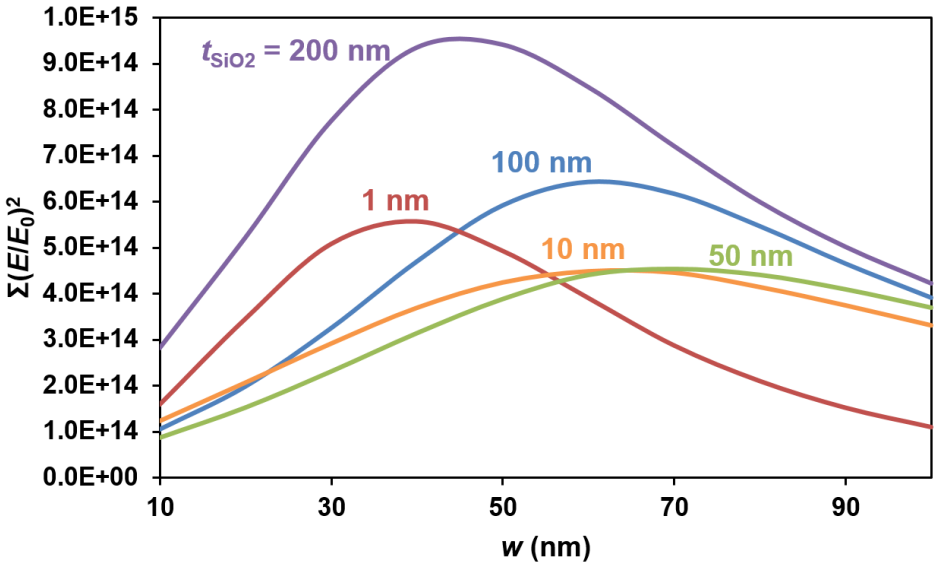

Figure 4. Plot of the summation of optical enhancement $(E/E_0)^2$ vs $w_1 = w_2 = w$ with data from the area of interest surrounding the model nanogap for various values of SiO_2 thickness.

The results shown in Figure 4 don't show a clear correlation between the peak optical enhancement at different Au widths and the thickness of the SiO_2 layer. While each plot displays a peak for the structure width shown, additional peaks may be present for larger Au widths, and the location of the peaks on the plot does not follow an obvious trend. It appears that there is a maximum enhancement for $t_{SiO2} = 200$ nm, but truly determining the optimal thickness will require more and larger parametric sweeps of various conditions. Future work for this study will require additional simulations in order to fully determine the effects of the oxide layer on the optical enhancement of the device. It is believed that a wavelength-dependent sinusoidal trend is likely to be found if one plots the enhancement versus t_{SiO2} for a large enough thickness range. Future work will simulate a wider range for t_{SiO2}, different wavelengths, and actual dual-width gratings instead of the $w_1 = w_2$ case.

3. CONCLUSION

In conclusion, a finite element model has been created for the simulation of dual-width plasmonic grating electromagnetic enhancement studies. The model has been utilized in the calculation of preliminary results demonstrating effects of varying the silicon dioxide thickness beneath the grating structure. The preliminary results of enhancement versus Au width for different SiO_2 thicknesses do not display an obvious correlation between peak enhancement and oxide layer thickness. Thus, future work will study a larger range of thicknesses with a finer step size. Other studies will include more geometrical parameter variations for combinations of Au structure widths and SiO_2 thickness, different incident light wavelengths, and determination of the potential benefits of dual-width structures over single width gratings. A newly developed Raman spectroscopy setup will also be used to experimentally characterize fabricated dual-width grating samples for comparison with the current computational optimization studies.

ACKNOWLEDGEMENTS

We would like to acknowledge the following colleagues at the University of Arkansas and elsewhere for all of their help and support: Zachary Brawley, Ahmad Nusir, Mourad Benamara, and Brandon Rogers. Funding for this research has been provided by the Department of Physics, the Fulbright College of Arts and Sciences, and the Vice Provost for Research and Economic Development at the University of Arkansas. Stephen J. Bauman has been supported by the Doctoral Academy Fellowship through the University of Arkansas Graduate School and the SPIE Optics + Photonics Education Scholarship.

REFERENCES

[1] Catchpole, K. R.., Polman, A., "Plasmonic solar cells," Opt. Express **16**(26), 21793 (2008).

[2] Pillai, S.., Green, M. A., "Plasmonics for photovoltaic applications," Sol. Energy Mater. Sol. Cells **94**(9), 1481–1486 (2010).

[3] Camden, J. P., Dieringer, J. A., Zhao, J.., Van Duyne, R. P., "Controlled Plasmonic Nanostructures for Surface-Enhanced Spectroscopy and Sensing," Acc. Chem. Res. **41**(12), 1653–1661 (2008).

[4] Rahbany, N., Geng, W., Blaize, S., Salas-Montiel, R., Bachelot, R.., Couteau, C., "Integrated plasmonic double bowtie / ring grating structure for enhanced electric field confinement," Nanospectroscopy **1**(1) (2015).

[5] Chen, X., Park, H.-R., Pelton, M., Piao, X., Lindquist, N. C., Im, H., Kim, Y. J., Ahn, J. S., Ahn, K. J., et al., "Atomic layer lithography of wafer-scale nanogap arrays for extreme confinement of electromagnetic waves," Nat. Commun. **4** (2013).

[6] Awang, R. A., El-Gohary, S. H., Kim, N.-H.., Byun, K. M., "Enhancement of field–analyte interaction at metallic nanogap arrays for sensitive localized surface plasmon resonance detection," Appl. Opt. **51**(31), 7437–7442 (2012).

[7] Chen, J., Qin, G., Wang, J., Yu, J., Shen, B., Li, S., Ren, Y., Zuo, L., Shen, W., et al., "One-step fabrication of sub-10-nm plasmonic nanogaps for reliable SERS sensing of microorganisms," Biosens. Bioelectron. **44**, 191–197 (2013).

[8] Bauman, S. J., Debu, D. T., Hill, A. M., Novak, E. C., Natelson, D.., Herzog, J. B., "Optical nanogap matrices for plasmonic enhancement applications," SPIE Proc **9163**, 91631A–91631A–6, International Society for Optics and Photonics, San Diego, CA (2014).

[9] Darweesh, A. A., Bauman, S. J., Brawley, Z.., Herzog, J., "Improved optical enhancement in binary plasmonic gratings with nanogap spacing," Manuscr. Prep. (2016).

[10] Siegfried, T., Ekinci, Y., Solak, H. H., Martin, O. J. F.., Sigg, H., "Fabrication of sub-10 nm gap arrays over large areas for plasmonic sensors," Appl. Phys. Lett. **99**(26), 263302 (2011).

[11] Chul Kim, H.., Cheng, X., "Gap surface plasmon polaritons enhanced by a plasmonic lens," Opt. Lett. **36**(16), 3082 (2011).

[12] Clark, A. W.., Cooper, J. M., "Nanogap Ring Antennae as Plasmonically Coupled SERRS Substrates," Small **7**(1), 119–125 (2011).

[13] Li, K., Jiang, K., Zhang, L., Wang, Y., Mao, L., Zeng, J., Lu, Y.., Wang, P., "Raman scattering enhanced within the plasmonic gap between an isolated Ag triangular nanoplate and Ag film," Nanotechnology **27**(16), 165401 (2016).

[14] Bauman, S. J., Darweesh, A. A.., Herzog, J. B., "Surface-enhanced Raman spectroscopy substrate fabricated via nanomasking technique for biological sensor applications," SPIE Proc **9759**, 97591I–97591I–8, International Society for Optics and Photonics, San Francisco, CA (2016).

[15] Guo, H.., Guo, J., "Hybrid plasmon photonic crystal resonance grating for integrated spectrometer biosensor," Opt. Lett. **40**(2), 249 (2015).

[16] Chiu, N.-F., Yang, C.-D., Kao, Y.-L.., Cheng, C.-J., "Design of plasmonic circular grating with broadband absorption enhancements," SPIE Proc **9502**, 950213-950213–950216, International Society for Optics and Photonics (2015).

[17] Homola, J., Koudela, I.., Yee, S. S., "Surface plasmon resonance sensors based on diffraction gratings and prism couplers: sensitivity comparison," Sens. Actuators B Chem. **54**(1–2), 16–24 (1999).

[18] Lin, K., Lu, Y., Chen, J., Zheng, R., Wang, P.., Ming, H., "Surface plasmon resonance hydrogen sensor based on metallic grating with high sensitivity," Opt. Express **16**(23), 18599 (2008).

[19] Bauman, S. J., Novak, E. C., Debu, D. T., Natelson, D.., Herzog, J. B., "Fabrication of Sub-Lithography-Limited Structures via Nanomasking Technique for Plasmonic Enhancement Applications," IEEE Trans. Nanotechnol. **14**(5), 790–793 (2015).

[20] Darweesh, A. A., Bauman, S. J.., Herzog, J. B., "Improved optical enhancement using double-width plasmonic gratings with nanogaps," Rev. (2016).